Collapse of Skin Antioxidant Status during the Subacute Period of Cutaneous Radiation Syndrome: A Case Report

Authors: Benderitter, Marc, Isoir, Muriel, Buard, Valérie, Durand, Valérie, Linard, Christine, et al.

Source: Radiation Research, 167(1) : 43-50

Published By: Radiation Research Society

URL: https://doi.org/10.1667/RR0577.1

RADIATION RESEARCH **167**, 43–50 (2007)
0033-7587/07 $15.00

Collapse of Skin Antioxidant Status during the Subacute Period of Cutaneous Radiation Syndrome: A Case Report

Marc Benderitter,[a,1] Muriel Isoir,[a] Valérie Buard,[a] Valérie Durand,[a] Christine Linard,[a] Marie Catherine Vozenin-Brotons,[a] Jean Steffanazi,[b] Hervé Carsin[b] and Patrick Gourmelon[a]

[a] *Laboratoire de RadioPathologie, SRBE, DRPH, IRSN, Fontenay-aux Roses, France; and* [b] *Centre de Traitement des Brûlés, HIA Percy, Clamart, France*

Benderitter, M., Isoir, M., Buard, V., Durand, V., Linard, C., Vozenin-Brotons, M. C., Steffanazi, J., Carsin, H. and Gourmelon, P. Collapse of Skin Antioxidant Status during the Subacute Period of Cutaneous Radiation Syndrome: A Case Report. *Radiat. Res.* 167, 43–50 (2007).

This case report describes a patient suffering from accidental cutaneous radiation syndrome. Clinical symptoms were characterized by the presence of moist epidermal denudation over approximately 8% of the body surface without signs of necrosis 88 days after radiation exposure. The skin transcriptional profile was obtained and provides a comprehensive overview of the changes in gene expression associated with skin wound healing after irradiation. In particular, our data show a specific set of genes, i.e. *SOD1, GPX1, TDX1, TDX2* and *HSP60,* implicated in the redox control of normal skin repair after radiation exposure, whereas *HOX1* and *HOX2* were involved in the pathological skin repair. A reduction in the antioxidant capacity of the irradiated tissue concomitant with a progressive establishment of an uncontrolled inflammatory response was noted. Our data corroborate the hypothesis that ROS modulation is a key element of the healing response after cutaneous exposure to radiation and that the collapse of skin antioxidant status interferes directly with wound healing in skin after radiation exposure. Thus a better understanding of the molecular events through which oxidative stress modulates the healing response could result in a more rational therapeutic approach to the pathological process induced after exposure of skin to radiation.

INTRODUCTION

The skin response to high-dose ionizing radiation may involve multiple inflammatory and necrotic outbreaks. This depends on the radiation dose and the volume of irradiated tissue as well as on the radiosensitivity of the patient (*1, 2*). Skin wound healing is a highly ordered process with major tissue movement resulting in rapid closure of the wound site and the subsequent regeneration of the injured tissue (*3*). Although protein-type mediators have a well-established role in this process, it has become evident that a modulation of the redox status is involved in wound healing (*4*).

A growing body of evidence supports a causative role of oxidative stress in the course of the tissue healing response after radiation exposure (*5*). Radiation-induced oxidative stress appears to result not only from ROS generated at the time of irradiation but also from the propagation of radicals occurring in the days after the irradiation. While there are currently no data directly demonstrating the presence of chronic oxidative stress in irradiated skin, indirect evidence in support of this hypothesis has come from studies using an antioxidant-based intervention. Thus administration of liposomal Cu/ZnSOD and MnSOD 6 months after irradiation in an experimental model of radiation-induced fibrosis has been shown to reverse the radiation-induced fibrosis and to allow the regeneration of normal tissue in an area of well-established postirradiation fibrosis (*6*). Similar results have been observed experimentally and clinically using a combination of pentoxifylline and the antioxidant α-tocopherol (*7*).

This paper illustrates, for the first time to our knowledge, how modulation of oxidative stress and inflammation are linked in the healing response after skin exposure to ionizing radiation. In many instances, during wound healing, ROS are key elements of the skin healing response to ionizing radiation.

PATIENTS AND METHODS

Patients

All clinical investigations were conducted in accordance with accepted ethical and humane practices as stated by the Declaration of Helsinki principles. Written consent was obtained from all patients.

The patient whose skin was examined in the present study suffered from an accidental whole-body exposure to X rays associated with a major cutaneous radiation syndrome characterized by an extensive moist epidermitis without necrosis. The radiological cutaneous syndrome in-

[1] Institut de Radioprotection et de Sûreté Nucléaire, Direction de la RadioProtection de l'Homme, Service de RadioBiologie et d'Epidémiologie, Laboratoire de RadioPathologie, IRSN, B.P. no. 17, F-92262 Fontenay-aux-Roses Cedex, France; e-mail: marc.benderitter@irsn.fr.

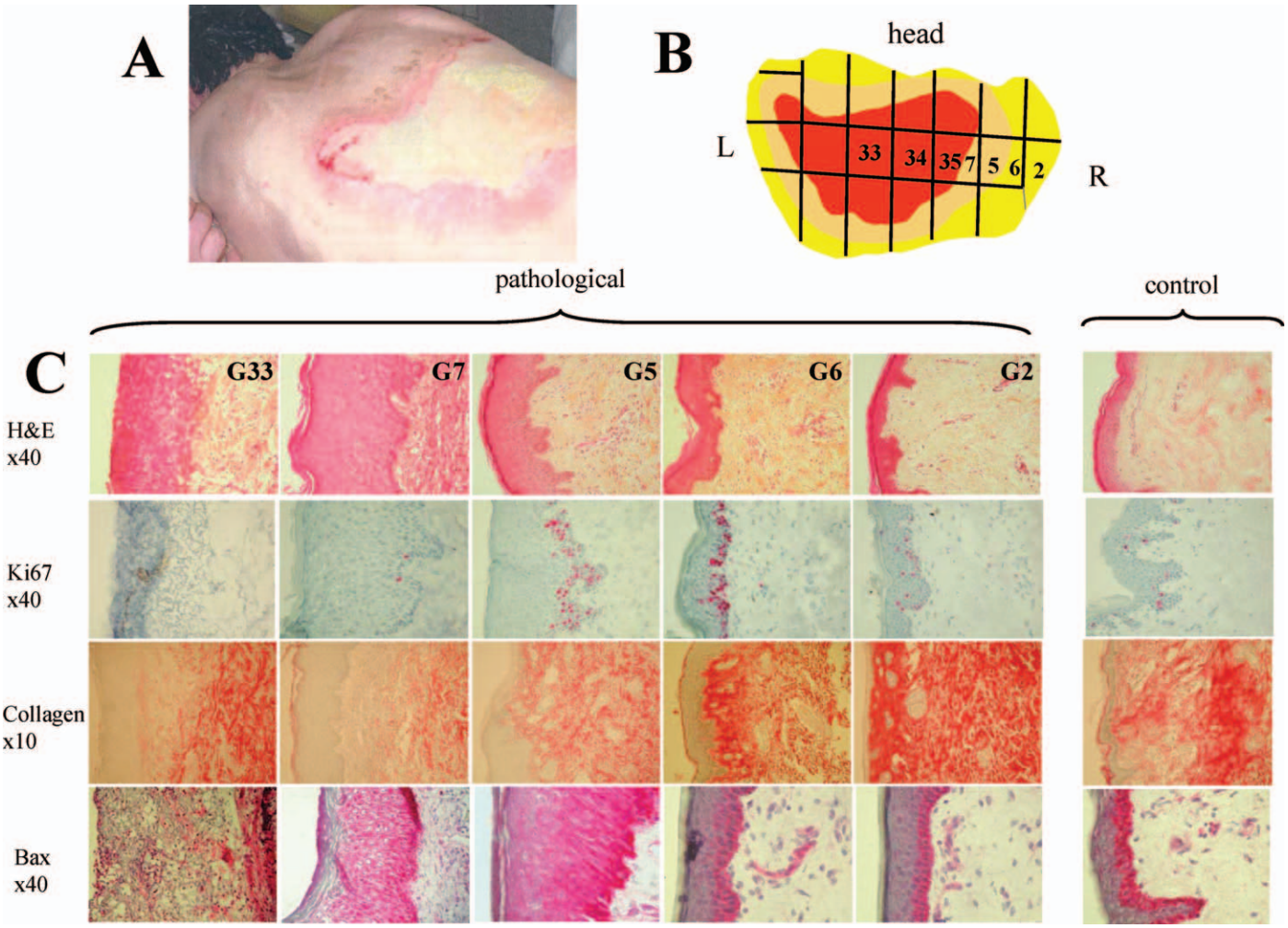

FIG. 1. Histological changes after human skin exposure to ionizing radiation. Panel A: Photograph of the lesion of the victim (radiological accident of Lia-Georgia). Panel B: Schematic representation of the lesion and position of the biopsies (G2 to G34). Panel C: H&E staining, Ki67 immunostaining, Sirius red staining and BAX immunostaining of skin biopsies as a function of the position in the skin lesion (G2 to G34).

volved the whole posterior side of the thorax from the waist up to the end point of the scapulae. Based on clinical signs and according to the medical staff in charge of the patient, three different concentric skin areas were defined. At the periphery of the skin lesion, a first area was defined as healthy. This area was exposed to X-ray doses lower than 5.2 Gy. Concentric and enclosed in this area, a second area characterized by ''normal healing'' tendency was defined. This inflamed area was exposed to X-ray doses ranging from 5.2 to 18.9 Gy. The third area was the center of the lesion. This area, i.e. the ''pathological wound healing area'', was the most exposed area (>25 Gy) and was characterized by an extensive moist epidermitis without healing tendency. Dose mapping was obtained according to the biological dosimetry procedure as described in our previous paper (*8*). The whole lesion including the three areas was excised surgically at day 88 after irradiation, and a skin graft was performed.

Excess surgical tissue from resected abdominal skin from three unirradiated patients (Caucasian men 35–45 years old) was obtained and used as controls.

Tissue Sampling

Additional small biopsies were taken from the excised skin of both central patients and the patient suffering from the radiological cutaneous syndrome (Fig. 1B). In both cases, some of the tissue samples were fixed in formalin and embedded in paraffin, while others were snap-frozen in liquid nitrogen and stored at −80°C.

Skin Histopathology

A primary histological examination of a 5-μm tissue section was performed by staining with hematoxylin and eosin (H&E) after fixation in 5% formaldehyde.

Skin RNA Extraction and Quality Control

Whole frozen tissue samples (epidermis and dermis) were crushed into powder under liquid nitrogen. Samples were then homogenized in 4 *M* guanidium thiocyanate using 1.2 gauss syringes. Total RNAs were purified according to the technique of Chomczynski and Sacchi after phenol/chloroform extraction. The RNA was treated with RNase-free DNase (0.5 U/μl) to remove contaminating genomic DNA. The success of the DNA digestion, in both quantity and quality (28S/18S ratio), of the RNAs extracted was determined for each sample using an Agilent 2100 Bioanalyzer (Agilent Technologies, Palo Alto, CA).

Skin mRNA Expression Analysis using cDNA Arrays

The gene expression analysis was performed through hybrid selection of radiolabeled cDNA on high-density arrays of membrane-bound cDNAs. The Atlas Human 1.2 (1176 genes + 9 housekeeping genes) cDNA expression array (Clontech Laboratories, Palo Alto, CA) was used for this experiment. PolyA+ RNA enrichment was obtained after column

chromatography by using a streptavidin magnetic bead preparation according to the Atlas Pure total RNA labeling system techniques (Clontech Laboratories). The cDNA was synthesized as described in the Atlas cDNA Expression Array kit and 370 kBq/μl [α-^{32}P]dATP was incorporated into synthesized cDNA. To purify the labeled cDNA from labeled ^{32}P nucleotides and small cDNA fragments, each sample was purified using column chromatography. The radioactivity of the probe was verified by scintillation counting (Beckman Coulter, Fullerton, CA). The cDNA probes were hybridized overnight (a 20-h incubation period was optimized to obtain an acceptable hybridization signal with high signal/background ratio and to avoid any signal covering a neighboring area) in the Atlas array with continuous agitation at 68°C. After the hybridized membrane was washed according to the Atlas cDNA expression array protocol, the Atlas array was removed from the container and wrapped in plastic wrap. The Atlas arrays were in contact with a phosphorimaging screen for 20 h at room temperature and revealed by using a Typhoon 9400 phosphorimager (Amersham Biosciences Europe, Freiburg, Germany). Comparisons between the different samples were made using BD Atlasimage 2.7 software (Clontech Laboratories). Four housekeeping genes were selected (phospholipase-2, gyceraldehyde-3 phosphate dehydrogenase, ribosomal protein L13a and tyrosine 3 monooxygenase/tryptophan 5 monooxygenase activation protein), and only the irradiated:control ratios above 2 and below 0.5 were taken into account.

Skin Differential Gene Expression as Confirmed by Real-Time PCR

To provide independent confirmation of the array data, real-time RT-PCR was performed on selected transcripts. Briefly, 2 μg of skin extract total RNA was reverse transcribed with Superscript II reverse transcriptase (Life Technology-Invitrogen, Cergy Pontoise, France) with 200 U of Superscript reverse transcriptase in a 20-μl reaction containing 1× Superscript buffer, 1 m*M* dNTP, 20 ng random hexamer, 10 m*M* DTT and 20 U of RNase inhibitor. This mixture was incubated for 50 min at 42°C and 10 min at 70°C. For TNFA and IL1B, primers from the manufacturer were used to amplify first-strand cDNA through 40 PCR cycles with TaqMan (Applied Biosystems, Foster City, CA). The PCR amplification of the other genes used the Syber PCR master Mix; the primer sequences purchased from Life Technology-Invitrogen (Cergy Pontoise, France), were as follows: MnSOD, 5′-GGTGGTCATATCAATCATAG-3′ (forward); 5′-AGTGGAATAAGGTTTGTTGT-3′ (reverse), Cu/ZnSOD, 5′-CAGTGCAGGTCCTCACTTTA-3′ (forward); 5′-CCTGTCTTTGTACTTTCTTC-3′ (reverse), catalase, 5′-TTAATCCATTCGATCTCACC-3′ (forward); 5′-GGCGGTGAGTGTCAGGATAG-3′ (reverse). Samples were subjected to 40 cycles of amplification at 95°C for 15 s, followed by 60°C for 1 min using ABI PRISM 7500 detection system (Applied Biosystems). Both water and genomic DNA controls were included to ensure specificity. PCR fluorescent signals were normalized to the signal obtained from the housekeeping gene 18s for each sample. All data were examined for integrity by analysis of the amplification plot and dissociation curves. Relative mRNA quantification was performed using the comparative $\Delta\Delta C_T$ method. Relative quantification in the skin biopsy was equal to $2^{-\Delta\Delta CT}$ (*10*). $\Delta\Delta C_T$ is defined as the difference between the mean ΔC_T (exposed skin) and the mean ΔC_T (healthy skin). ΔC_T is defined as the difference between the mean C_T (antioxidant enzyme) and C_T (18s), which is the endogenous control in our experiment.

Skin Immunostaining

Five-micrometer sections were cut using a cryostat (OTF, Bright, England) at −30°C. Frozen sections were fixed with either paraformaldehyde (0.5%, 30 min) or acetone (4°C, 10 min). Sections were then permeabilized with Triton X-100 (0.1%, 20 min), washed in PBS, and saturated with PBS/BSA solution (2%). The sections were then incubated overnight (4°C) with two different antibodies [CD 3 T cell (DAKO, Trappe, France), MPO (Novocastra Laboratory, Newcastle upon Tyne, UK)]. Immunostaining was performed using a Nexes IHC automated immunostainer (Ventana, Illkirch, France). The sections were fixed [glutaraldehyde (0.05%, 4 min, 37°C)], incubated with goat anti-mouse antibody and then incubated with streptavidin-alkaline phosphatase, Fast Red and naphthanol. Sections were counterstained with hematoxylin. The sections were mounted in PBS-glycerol (50%) and examined with an epifluorescence microscope. A semi-quantitative approach using an image analyzer Visioscan (Biocom, Paris, France) was chosen. Ten different fields were measured on each slide, and six different slides were analyzed for each region.

Measurement of Skin Antioxidant Defenses

Tissue samples stored at −80°C were homogenized in pH 7.5 phosphate buffer with an ultra-turrax (IKA Labortechnick, Munchen, Germany) at 4°C. The skin homogenate was then centrifuged, and the supernatant was evaluated for protein content using the Coomassie protein assay. The decomposition of hydrogen peroxide catalyzed by catalase contained in the skin homogenate supernatant was followed spectrophotometrically at 240 nm on a Uvikon 840 (Biotek-Kontron, Saint Quentin en Yvelines, France). The H_2O_2 concentration was adjusted spectrophotometrically at 240 nm. The activity was measured from the slope of the line as micromoles of H_2O_2 decomposed per minute per milligrams of protein. Glutathione peroxidase activity was measured by a standard coupled assay procedure. The reaction mixture consisted of phosphate buffer (0.5 *M,* pH 7.0), 3.12 m*M* EDTA, 12.5 m*M* KCN, 0.005 m*M* glutathione, 0.86 m*M* NADPH, H^+ and 0.25 IU ml^{-1} glutathione reductase. Erythrocyte hemolysate was added to the above mixture and was incubated for 15 min at 30°C before initiation of the reaction by addition of 100 μl tert butyl hydroperoxide. Absorption at 340 nm was recorded for 10 min on a Uvikon 840. The activity was calculated from the slope as micromoles of NADPH oxidized per minute. The total SOD was quantified in the skin homogenate supernatant by its capacity to inhibit the reduction of nitro blue tetrazolium (0.012 μ*M*) by superoxide, which was produced by a xanthine (0.02 m*M*)/xanthine oxidase (0.1775 IU/ml) system at 30°C. The appearance of reduced NBT was monitored at 560 nm on a Uvikon 840. SOD prevents the reduction of NBT by superoxide and decreases the slope of the curve for the appearance of reduced NBT proportionally. The supernatant of the skin homogenate was diluted 1/10 to ensure a decrease in the slope between 20 and 30%. To determine the MnSOD activity, the assay was carried out in the presence of 1 mmol/liter potassium cyanide. The Cu/ZnSOD activity was obtained by subtracting the value for MnSOD from that of the total SOD.

Skin Cytokine Content

Tissue samples stored at −80°C were homogenized in phosphate buffer containing a protease inhibitor cocktail using an Ultra Turrax at 4°C. The skin homogenate was then centrifuged and the protein content of the supernatant was evaluated using a Coomassie protein assay. IL1B, IL6, IL8, TNFA, IL1RA and IL10 levels were measured in the supernatant by specific ELISA according the manufacturer's recommendation (R&D Systems, Abingdon, UK). The cytokine content was determined by specific ELISA according to the manufacturer's recommendations

Statistical Methods

All results are expressed as means ± the standard errors of the means (SEM) for duplicate skin biopsies from three different healthy patients and for duplicates of three different skin biopsies from the irradiated patient. Significance tests used an ANOVA associated with Dunn's or Dunnett's tests. Significance was set at $P < 0.05$.

RESULTS

Ionizing Radiation Induces Specific Morphological Changes as Revealed by the Histological Examination

The examination of H&E sections (Fig. 1C) revealed common histological features of moist desquamation, de-

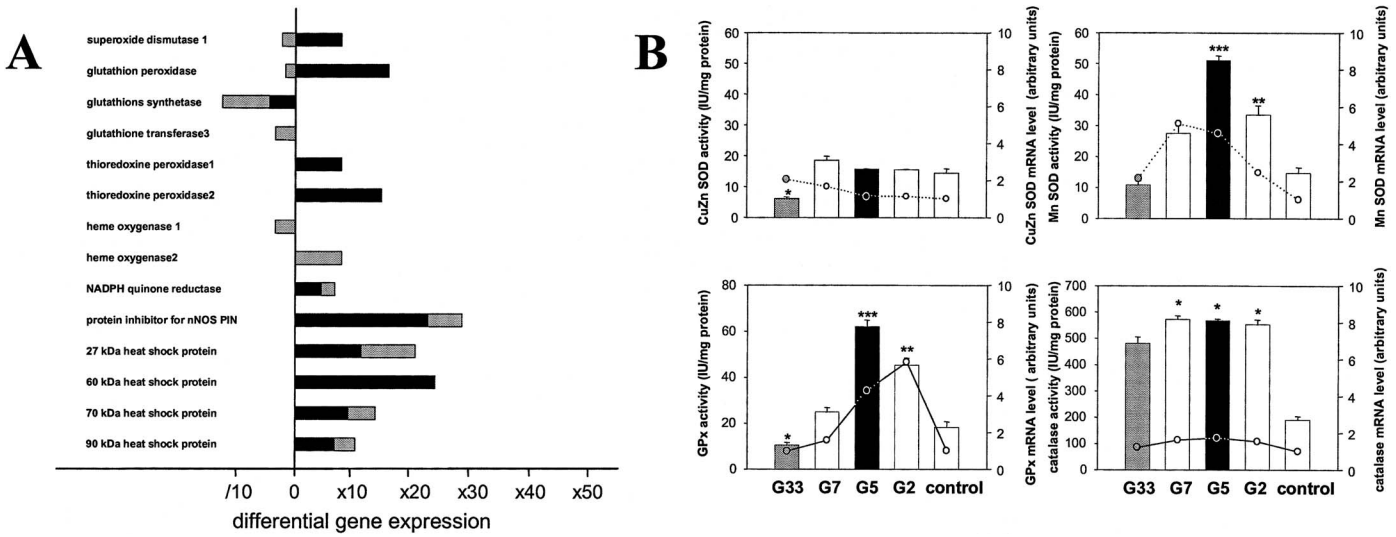

FIG. 2. Collapse of antioxidant status during skin pathological wound healing. Panel A: Differential redox gene expression after exposure of human skin to ionizing radiation. Tissue mRNAs were extracted and corresponding cDNAs were hybridized on Atlas cDNA expression arrays. Gene expressions were normalized to normal healthy skin (pool of three different human skin biopsies). G5 (black horizontal columns) and G33 (gray horizontal columns) refer to the position of the skin biopsy according to Fig. 1. Gene expression was significantly up-regulated (×) when the ratio was above 2 and significantly down-regulated (/) when the ratio was lower than 0.5. Panel B: Confirmation of the differential redox gene expression by real-time PCR (line plots: right *y* axis) (gene expression is normalized relative to normal healthy skin) and by enzymatic activity measurement (vertical bar plots: left *y* axis). G5 (black vertical columns and black circles), G33 (gray vertical columns and gray circles) and control, G2 and G7 (white vertical columns and white circles) refer to the position of the skin biopsy according to Fig. 1. Results are expressed as the means ± SEM ($n = 6$ per skin biopsy). $*P < 0.5$, $**P < 0.01$, $***P < 0.001$ compared with control skin.

pending on the position within the skin lesion. Marked epidermolysis associated with a loss of adhesion of the epidermis to the basal layer and microvascular destruction was observed in the center of the lesion. The lack of dermal necrosis, as noted after examination of H&E-stained sections, was confirmed by BAX immunohistochemical staining (Fig. 1C). Also, the epidermal hyperproliferative response measured using Ki67, the perivascular inflammatory cell infiltration, and the extracellular matrix protein deposition, i.e. collagen, revealed a healing process surrounding the lesion (Fig. 1C).

Ionizing Radiation Induces a Specific Set of Genes as Revealed by the cDNA Array Technique

The intensity of the arrays from the healthy skin (pool of three different human skin biopsies) was averaged and compared with the intensity of arrays from two different irradiated areas. The first area sampled was located in the ''healthy area'' (position G5; see the Patients and Methods section and Fig. 1B) and the second was located in the ''pathological healing area'' (position G33; see Patient and Methods section and Fig. 1B). The differentially expressed genes represent 11% (145/1314) of the genes spotted on the membrane, including mainly genes involved in the control of the cellular redox status (Fig. 2) and in the control of the inflammatory response (Fig. 3).

Collapse of Skin Antioxidant Status during Pathological Wound Healing after Radiation Exposure

Skin gene array analysis. The expression of genes usually involved in the control of the cellular redox status including *SOD1, GPX1* and Thioredoxin 1 and 2 was increased in the normal healing skin, whereas GSH synthetase was decreased. The protein inhibitor for nNOS (PIN) was found to be highly overexpressed in normal healing skin. All these genes were not expressed in the pathological healing area, whereas genes coding for heme oxygenase 1 and 2 were found to be specifically overexpressed in pathological healing skin. The stress response in both the normal and the pathological healing areas was also characterized by an increase in the expression of genes encoding for heat-shock proteins HSP27, HSP70 and HSP90. The gene encoding for HSP60 was highly and specifically expressed in normal healing skin but not in pathological healing skin (Fig. 2A).

Real-time PCR analysis of skin gene expression. The validation of gene modulations of some representative antioxidant enzymes (Fig. 2B), as observed by the microarray technique, was performed by real-time RT-PCR. The results obtained by these two techniques were correlated. The gene expression of antioxidant enzymes (MnSOD, Cu/ZnSOD, GPX), as measured by RT-PCR was found to be significantly and gradually up-regulated at a position in the center of the skin lesion when compared to the control area. Catalase gene expression remained stable in the various samples. In the center of the lesion (position G33), a decrease in gene expression was confirmed (Fig. 2B). HSP27 gene expression, as measured by RT-PCR, was significantly up-regulated independently of the position in the skin lesion (not shown).

Skin antioxidant enzyme activity measurement. Antioxidant enzyme activities were increased significantly and

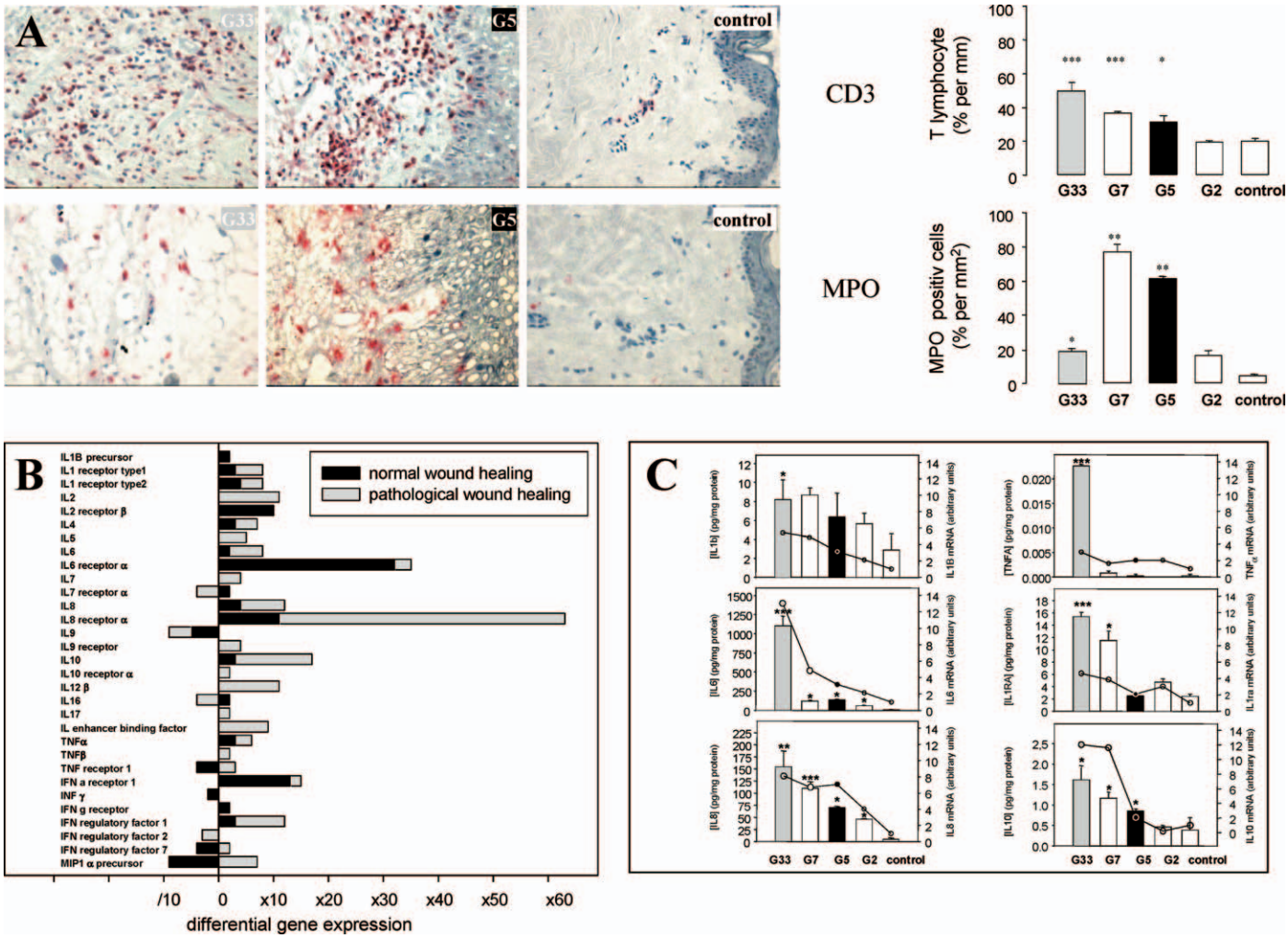

FIG. 3. Chronic inflammatory response during skin pathological wound healing. Panel A: Left frame: Immunohistochemistry showing inflammatory cell infiltration after radiation exposure [T lymphocytes (CD3), neutrophils (myeloperoxidase)]. Original magnification 10× for G33 and G7 and 40× for control. Right frame: Quantification of the inflammatory cell infiltration. G5 (black columns), G33 (gray columns) and control, G2 and G7 (white vertical columns) refer to the position of the skin biopsy according to Fig. 1. Data are expressed as means ± SEM ($n = 6$ per skin biopsy). $*P < 0.5$, $**P < 0.01$, $***P < 0.001$ compared to control skin. Panel B: Differential inflammatory gene expression after exposure of human skin to ionizing radiation. Tissue mRNAs were extracted and corresponding cDNAs were hybridized on Atlas cDNA expression arrays. Gene expressions were normalized to normal healthy skin (pool of three different human skin biopsies). G5 (black horizontal columns) and G33 (gray horizontal columns) refer to the position of the skin biopsy according to Fig. 1. Gene expression was significantly up-regulated (×) when the ratio was above 2 and significantly down-regulated (/) when the ratio was lower than 0.5. Panel C: Confirmation of the differential inflammatory gene expression by real-time PCR (line plots: right *y* axis) (gene expressions are normalized to normal healthy skin) and by ELISA quantification of skin cytokines (IL1B, TNFA, IL6, IL1RA, IL8, IL10; vertical bar plots: left *y* axis). G5 (black vertical columns and circles), G33 (gray vertical columns and circles) and control, G2 and G7 (white vertical columns and white circles) refer to the position of the skin biopsy according to Fig. 1. Results are expressed as means ± SEM ($n = 6$ per skin biopsy). $*P < 0.5$, $**P < 0.01$, $***P < 0.001$ compared with control skin.

gradually in the normal healing skin [67% increase in MnSOD activity ($P = 0.0102$), 247% increase in GPX activity ($P = 0.0095$), and 143% increase in catalase activity ($P = 0.028$) comparing the G5 position to control skin]. Cu/ZnSOD activity remained unchanged. In the pathological healing skin (position G33), a significant reduction in antioxidant enzyme activities was observed [58% decrease in Cu/ZnSOD activity ($P = 0.021$), 47% decrease in GPX activity ($P = 0.048$) comparing the G33 position to control skin] (Fig. 2B). Unlike the other antioxidant enzyme assayed, catalase and MnSOD activities did not decrease in the pathological healing skin.

Interrelationship of Skin Redox Modulation and Skin Inflammatory Response to Ionizing Radiation

Skin inflammatory cell infiltration. Basal values of 19.7 ± 1.8% for T lymphocytes and 3.2 ± 0.7% for neutrophils were found using CD3 and MPO immunodetection, respectively, in control human skin (Fig. 3A). After radiation exposure, perivascular infiltration of inflammatory cells was noted. Cell infiltration increased significantly as a function of the position within the lesion. A statistically significant increase in T-lymphocyte infiltration was observed from position G5 at the edge of the lesion (a 1.8-fold in-

crease compared to the control, $P = 0.43$) to position G33 in the center of the lesion (a 2.6-fold increase compared to the control, $P = 0.0071$) (Fig. 3A). A significant increase in neutrophil infiltration was also observed and quantified from position G2 to G7 in the edge of the lesion (20-fold increase compared to the control, $P = 0.057$). A drop in neutrophil infiltration was noted in the center of the lesion (Fig. 3A). Interestingly, the MPO degranulation in the area corresponding to positions G5 and G7 probably corresponds to neutrophil activation (Fig. 3A).

Skin gene array analysis. Expression of genes for the pro-inflammatory cytokines, i.e. IL1B, IL6, IL8 and TNFA, increased after radiation exposure in both normal and pathological healing skin. Gene expression of anti-inflammatory cytokines, i.e. IL1R1, IL4 and IL10, also increased in both normal and pathological healing skin. Up-regulation of genes coding for IL2RB, IL7RA and IFNGR corresponds to the specific inflammatory gene expression pattern of normal healing. Up-regulation of genes coding for IL2, IL5, IL7, IL9R, IL10RA, IL12B, IL17, TNFB and MIP1A and down-regulation of genes coding for IL7RA, IL9, IL16 and IRF2 corresponds to the specific inflammatory gene expression pattern of pathological skin (Fig. 3B).

Real-time PCR analysis. The validation of up-regulations of gene for analysis, representative cytokines (Fig. 3C), as observed by gene array, was obtained by real-time RT-PCR. The expression of pro-inflammatory (IL1B, IL6, IL8, TNFA) and anti-inflammatory cytokine (IL1RA, IL10) genes was quantified. Again, the levels of gene expression, as assessed by RT-PCR, were similar to those obtained by gene array analysis. A correlation between these two techniques was observed for each position examined within the lesion. All gene up-regulations were confirmed to be increased significantly and gradually as a function of the position within the skin lesion when compared to control area, except for TNFA (Fig. 3C).

Skin cytokine level. The inflammatory cytokine level increased significantly in the center of the lesion (position G33) when considering both pro-inflammatory cytokines [5.6-fold increase of IL1B ($P = 0.0023$), 98-fold increase of IL6 ($P = 0.001$), 65-fold increase of IL8 ($P = 0.0095$), and 89-fold increase of TNFA ($P = 0.00087$)] and anti-inflammatory cytokines [5.4-fold increase of IL1RA ($P = 0.017$) and 17-fold increase of IL10 ($P = 0.034$)] when comparing cytokine expression at the G33 position to that in control skin (Fig. 3C).

Radiation-Induced Modulation of Intracellular and Nuclear Signaling

Involvement of classical intracellular redox-sensitive signaling was observed using the array technique. It was interesting to note the modulation of gene expression of the homeobox family in the skin after radiation exposure. Expression of the genes encoding HOXA5, B5 and B7 was up-regulated in both normal and pathological healing skin.

TABLE 1
Differential Gene Expression in Irradiated Human Skin (Transcriptional Regulation)

GenBank	Gene	G5	G33
J 03133	Sp1 transcription factor	×4	×29
X 56681	AP1/Jun	×6	×20
L 26318	JNK1	×2	×2
AF 05216	JNK2	×4	×5
L 36870	JNKK1	/5	×4
AF 22805	JNKK2	×6	×21
AF 44195	RELA/NFKB	×2	×5
U 02683	nuclear respiratory factor 1	×2	×2
M 86546	homeox protein PBX1		×26
M 26679	homeobox A5	×5	×35
M 92299	homeobox B5	×25	×7
M 16937	homeobox B7	×2	×4
M 97676	homeobox MSX1	/3	×3

Notes. Data are expressed relative to normal healthy skin (pool of three different human skin biopsies). Normal wound healing corresponds to three different biopsies in the G5 area, and pathological wound healing corresponds to three different biopsies in the G33 area. Results were corrected by taking into account four different housekeeping genes (*PLA2*, *GAPDH*, *RPL13A* and tyrosine 3 mono oxygenase). Gene expression was significantly was significantly up-regulated (×) when the ratio was above 2 and significantly down-regulated (/) when the ratio was lower than 0.5.

A 25-fold increase was noted for HOXB5 for normal healing skin. Increases of 26- and 35-fold were observed for PBX1 and HOXA5, respectively, in pathological skin (Table 1).

DISCUSSION

The pathophysiological mechanisms that govern wound healing of skin exposed to ionizing radiation remain unclear, particularly during the subacute period (*9*). The present study suggests that a genome-wide gene expression analysis of irradiated skin can be an effective tool to improve the understanding of the pathophysiological mechanisms involved in the cutaneous radiation syndrome (*11*).

In particular, this approach highlights the importance of a specific set of the genes controlling the skin redox status that may interfere with normal skin wound healing. Up-regulation of *SOD1, GPX1, TDX1, TDX2* and *HSP27* was noted in the healing skin areas, whereas non-healing skin areas were characterized by both down-regulation of *SOD1, GPX1, TDX1, TDX2* and *HSP27* and up-regulation of *HOX1* and *HOX2*. Modulations of some of the most representative molecules of these different sets of genes were validated both by real-time PCR and measurements of enzymatic activity. To our knowledge, this is the first report of such a global investigation of skin redox status after exposure of human skin to radiation. Two complementary investigations were published recently on human keratinocytes (*12, 13*) and human fibroblasts (*14*) exposed *in vitro* to γ rays. However, it is difficult to compare these studies to ours given that *in vivo* the tissue context and architecture

are described as being able to modulate the cell response and result in a response that differs from the response of isolated cells *in vitro* to damage (*15*). Nevertheless, the results of the present investigation of human skin are in agreement with the observation of Jagetia *et al.* (*16*), particularly concerning the decrease in both SOD and GPX activities after high-dose exposure of skin. According to these authors, γ irradiation of mouse skin at doses ranging from 0 to 20 Gy resulted in a dose-dependent decrease in the activity of SOD and GPX.

Our data show that the collapse of skin antioxidant status is concomitant with a massive and uncontrolled infiltration of inflammatory cell in the skin. Feedback redox control was described as modulating the inflammatory response (*17, 18*). For that reason, the skin inflammatory cytokine pattern was investigated further. Skin pro-inflammatory cytokines (IL6, IL8, MCP1, TNFA, IFNG) were found to increase at both the mRNA and protein levels. Compensatory skin anti-inflammatory cytokine (IL4, IL10 or IL1RA) production was also noted at both the mRNA and protein levels. Interestingly, a gradient of the inflammatory response as a function of the position in the damaged tissue was observed. The perivascular neutrophil, macrophage and lymphocyte infiltrations observed in the lesion are accompanied by an epidermal infiltration in the area of intense epidermitis. This corresponds to a classic histological pattern of the cutaneous radiation syndrome (*19*). Some reports focused on the role of specific inflammatory cytokines like IL1 (*20*), IL6 (*21*) or IFNG (*22*) and concluded that there is prevalence of pro-inflammatory cytokines in the cutaneous radiation syndrome in human skin. Our cDNA array approach reinforces the importance of these candidate cytokines in the progression of the cutaneous syndrome. The data obtained by our cDNA array show how radiation exposure ultimately compromises tissue integrity by altering the cytokine network among skin cells and underscores the complexity of this biological response. A Th2 cytokine profile (IL4, IL10, IL13) was the dominant skin response in the irradiated area. This Th2 polarization favors a nonresolution of the inflammatory response (*23*) and probably contributes to the progression of the skin to a non-healing response.

Close interactions between oxidative stress and inflammation, as suggested by our study, have been described elsewhere in the literature through the involvement of different redox-sensitive transcription factors (*24*). ROS have a paradoxical role, exerting either a positive or negative effect on damage removal, and on inflammation in particular (*25*).

On the one hand, a low ROS concentration regulates cellular signaling pathways. Our present results suggest increased expression of redox-sensitive transcription factor SP1 (×29), AP1/JUN (×20), RELA/NFKB (×5) or NRF1 (×2), which are known to be involved in the transcriptional control of inflammatory cytokines (*26, 27*). However, feedback control of the redox modulation of inflammatory cytokines by the cytokines themselves is possible. Cytokines have been clearly described to modulate gene expression of antioxidant enzymes, particularly MnSOD (*30, 31*). The specific promoter structure seemed to be relevant for the control of tissue MnSOD gene expression and involves functional cooperation between SP1 and AP2 (*32*) in coordination with NFKB (*33, 34*). NFKB is actively involved in the up-regulation of the GPX and CAT in response to oxidative stress (*35*). Our cDNA array data strongly suggest that the inflammatory response appears to be a redox counterbalance in the healing skin area.

On the other hand, in the center of the lesion, inflammation becomes massive and chronic, as shown by our data. The tissue chronically releases inflammatory mediators and cytokine/chemokines such as tumor necrosis factor, interleukin 1 and interleukin 8, which induce neutrophil recruitment, thereby augmenting tissue damage (*29*). For that reason, ROS production becomes excessive and chronic so that ROS no longer acts as a biological regulator of the skin healing response but becomes deleterious.

It is interesting to note the extensive modulation of the homeobox gene family. These genes were first described as modulating embryogenesis (*28*). In recent years, they have also been described as participating in tissue remodeling (*27*). Particularly, *HOXB5* was shown to be redox-sensitive (*26*). The strong *HOXB5* up-regulation observed in the healing skin area was deficient in the non-healing skin area.

In conclusion, our hypothesis, validated here, is that chronic oxidative stress may drive the progression of skin healing after radiation exposure during the latent phase of the cutaneous radiation syndrome. The imbalance between the skin redox status and the inflammatory status probably contributes to the ''pathological'' wound healing of irradiated skin. We contend that the role of ROS in modulating inflammation should be considered when designing treatment protocols to accelerate tissue repair. A better understanding of the molecular events whereby oxidative stress modulates the healing response could result in a more rational therapeutic approach to the pathological process induced after skin exposure to radiation.

ACKNOWLEDGMENTS

This work was supported by Electricité de France and by the Direction Générale de l'Armement (research contract DGA no. 03 34 050).

Received: February 8, 2006; accepted: August 28, 2006

REFERENCES

1. J. W. Denham, M. Hauer-Jensen and L. J. Peters, Is it time for a new formalism to categorize normal tissue radiation injury? *Int. J. Radiat. Oncol. Biol. Phys.* **50**, 1105–1106 (2001).
2. P. Gottlöber, G. Krähn and R. U. Peter, Cutaneous radiation syndrome: Clinical features, diagnosis and therapy. *Hautarzt* **51**, 567–574 (2000).
3. S. Werner and R. Grose, Regulation of wound healing by growth factors and cytokines. *Physiol. Rev.* **83**, 835–870 (2003).

4. C. K. Sen, The general case for redox control of wound repair. *Wound Repair Regen.* **11**, 431–438 (2003).
5. M. E. Robbins and W. Zhao, Chronic oxidative stress and radiation-induced late normal tissue injury. *Int. J. Radiat. Biol.* **80**, 251–219 (2004).
6. M. C. Vozenin-Brotons, V. Sivan, N. Gault, C. Renard, C. Geffrotin, S. Delanian, J. L. Lefaix and M. T. Martin, Antifibrotic action of Cu/Zn SOD is mediated by TGF-β1 repression and phenotypic reversion of myofibroblasts. *Free Radic. Biol. Med.* **30**, 30–42 (2001).
7. S. Delanian and J. L. Lefaix, The radiation-induced fibroatrophic process: Therapeutic perspective via the antioxidant pathway. *Radiother. Oncol.* **73**, 119–131 (2004).
8. J. P. Pouget, C. Laurent, M. Delbos, M. Benderitter, I. Clairand, F. Trompier, J. Stephanazzi, H. Carsin, F. Lambert and P. Gourmelon, PCC-FISH in skin fibroblasts for local dose assessment: Biodosimetric analysis of a victim of the Georgian radiological accident. *Radiat. Res.* **162**, 365–376 (2004).
9. J. W. Denham and M. Hauer-Jensen, The radiotherapeutic injury—a complex 'wound'. *Radiother. Oncol.* **63**, 129–145 (2002).
10. K. J. Livak and T. D. Schmittgen, Analysis of relative gene expression data using real-time quantitative PCR and the $2(-\Delta\Delta C_T)$. *Method. Methods* **25**, 402–408 (2001).
11. M. Kunz, S. M. Ibrahim, D. Koczan, S. Scheid, H. J. Thiesen and G. Gross, DNA microarray technology and its applications in dermatology. *Exp. Dermatol.* **10**, 593–606 (2004).
12. M. Koike, Y. Ninomiya and A. J. Koike, Characterization of ATF3 induction after ionizing radiation in human skin cells. *J. Radiat. Res.* **46**, 379–385 (2005).
13. N. Franco, J. Lamartine, V. Frouin, P. Le Minter, C. Petat, J. J. Leplat, F. Libert, X. Gidrol and M. T. Martin, Low-dose exposure to gamma rays induces specific gene regulations in normal human keratinocytes. *Radiat. Res.* **163**, 623–635 (2005).
14. L. H. Ding, M. Shingyoji, F. Chen, J. J. Hwang, S. Burma, C. Lee, J. F. Cheng and D. J. Chen, Gene expression profiles of normal human fibroblasts after exposure to ionizing radiation: A comparative study of low and high doses. *Radiat. Res.* **164**, 17–26 (2005).
15. C. M. Nelson and M. J. Bissell, Modeling dynamic reciprocity: Engineering three-dimensional culture models of breast architecture, function, and neoplastic transformation. *Semin. Cancer Biol.* **15**, 342–352 (2005).
16. G. C. Jagetia, G. K. Rajanikant, S. K. Rao and M. S. Baliga, Alteration in the glutathione, glutathione peroxidase, superoxide dismutase and lipid peroxidation by ascorbic acid in the skin of mice exposed to fractionated gamma radiation. *Clin. Chim. Acta* **332**, 111–121 (2003).
17. S. Briganti and M. Picardo, Antioxidant activity, lipid peroxidation and skin diseases. What's new. *J. Eur. Acad. Dermatol. Venereol.* **17**, 663–669 (2003).
18. B. Khodr and Z. Khalil, Modulation of inflammation by reactive oxygen species: Implications for aging and tissue repair. *Free Radic. Biol. Med.* **30**, 1–8 (2001).
19. M. Steinert, M. Weiss, P. Gottlober, D. Belyi, O. Gergel, V. Bebeshko, N. Nadejina, I. Galstian, G. Wagemaker and R. U. Peter, Delayed effects of accidental cutaneous radiation exposure: Fifteen years of follow-up after the Chernobyl accident. *J. Am. Acad. Dermatol.* **49**, 417–423 (2003).
20. U. Behrends, R. U. Peter, R. Hintermeier-Knabe, G. Eissner, E. Holler, G. W. Bornkamm, S. W. Caughman and K. Degitz, Ionizing radiation induces human intercellular adhesion molecule-1 *in vitro*. *J. Invest. Dermatol.* **103**, 726–730 (1994).
21. A. Beetz, G. Messer, T. Oppel, D. van Beuningen, P. U. Peter and P. Kind, Induction of interleukin 6 by ionizing radiation in a human epithelial cell line: Control by corticosteroids. *Int. J. Radiat. Biol.* **72**, 33–43 (1997).
22. P. Gottlober, M. Steinert, W. Bahren, L. Weber, H. Gerngross and R. U. Peter, Interferon-gamma in 5 patients with cutaneous radiation syndrome after radiation therapy. *Int. J. Radiat. Oncol. Biol. Phys.* **50**, 159–166 (2001).
23. C. F. Anderson, S. Mendez and D. L. Sacks, Nonhealing infection despite Th1 polarization produced by a strain of Leishmania major in C57BL/6 mice. *J. Immunol.* **174**, 2934–2941 (2005).
24. I. Rahman and W. MacNee, Regulation of redox glutathione levels and gene transcription in lung inflammation: Therapeutic approaches. *Free Radic. Biol. Med.* **28**, 1405–1420 (2000).
25. K. J. Davies, Oxidative stress, antioxidant defences and damage removal, repair and replacement systems. *IUBMB Life* **50**, 279–289 (2000).
26. C. K. Galang and C. A. Hauser, Cooperative DNA binding of the human HoxB5 (Hox-2.1) protein is under redox regulation *in vitro*. *Mol. Cell Biol.* **13**, 4609–4617 (1993).
27. L. A. Uyeno, J. A. Newman-Keagle, I. Cheung, T. K. Hunt, D. M. Young and N. Boudreau, Hox D3 expression in normal and impaired wound healing. *J. Surg. Res.* **100**, 46–56 (2001).
28. E. J. Stelnicki, L. G. Komuves, A. O. Kwong, D. Holmes, P. Klein, S. Rozenfeld, H. J. Lawrence, N. S. Adzick, M. Harrison and C. Largman, HOX homeobox genes exhibit spatial and temporal changes in expression during human skin development. *J. Invest. Dermatol.* **110**, 110–115 (1998).
29. B. Khodr and Z. Khalil, Modulation of inflammation by reactive oxygen species: Implications for aging and tissue repair. *Free Radic. Biol. Med.* **30**, 1–8 (2001).
30. Y. Morel and R. Barouki, Repression of gene expression by oxidative stress. *Biochem. J.* **342**, 481–496 (1999).
31. M. I. Darville, Y. S. Ho and D. L. Eizirik, NF-kB is required for cytokine-induced manganese superoxide dismutase, expression in insulin-producing cells. *Endocrinology* **141**, 153–162 (2000).
32. Y. Xu, S. Porntadavity and D. K. St. Clair, Transcriptional regulation of the human manganese superoxide dismutase gene: The role of specificity protein 1 (Sp1) and activating protein-2 (AP-2). *Biochem. J.* **362**, 401–412 (2002).
33. G. Guo, Y. Yan-Sanders, B. D. Lyn-Cook, T. Wang, D. Tamae, J. Ogi, A. Khaletskiy, Z. Li, C. Weydert and J. J. Li, Manganese superoxide dismutase-mediated gene expression in radiation-induced adaptive responses. *Mol. Cell Biol.* **23**, 2362–2378 (2003).
34. L. Z. Zhou, A. P. Johnson and T. A. Rando, NFkB and AP-1 mediate transcriptional responses to oxidative stress in skeletal muscle cells. *Free Radic. Biol. Med.* **31**, 1405–1416 (2001).
35. S. A. Comhair and S. C. Erzurum, The regulation and role of extracellular glutathione peroxidase. *Antioxid. Redox Signal* **7**, 72–79 (2005).